

Photomicrography of Electrically Sprayed Heavy Particles

CHARLES D HENDRICKS JR,* RALPH S CARSON,† JAMES J HOGAN,† AND JOHN M SCHNEIDER†
University of Illinois, Urbana, Ill

One of the methods used to produce charged droplets, based on the electrical spraying of liquids from the tip of a conducting capillary tube, is briefly described. High-speed photomicrographs are shown which reveal details of the spraying mechanism at atmospheric pressure and at a pressure of about 10^{-5} torr for both stationary and pulsed conditions. The pictorial evidence is interpreted and discussed in terms of the physical constants of the liquids and the external parameters. Distributions of specific charge for several different liquids are presented and discussed briefly. The possibility of predicting and controlling the specific-charge distribution by electrical means is examined and recent achievements presented.

Introduction

PRELIMINARY analysis of space-flight trajectories has shown¹⁻³ that electrostatic thrust devices using particles with charge-to-mass ratios (specific charge) in the range of 10^2 – 10^5 coul/kg would permit achievement of payload optimization quite readily. In addition, beam neutralization problems would be minimized. The research discussed in this paper is presently aimed at furthering the general knowledge of charged droplet production and behavior by studying the effects of such physical properties as density, viscosity, conductivity, and surface tension on the specific-charge distribution. In this paper, high-speed photomicrographs of surface instabilities are presented and discussed, and Rayleigh's theory on the instability of charged droplets⁴ is extended to include droplet emission.

Electrical Spraying

Electrical spraying of liquids is the process whereby an externally applied electric field causes a dispersion of a quantity of the liquid into small discrete droplets. Any mechanical spraying that occurs in the absence of an electric field is therefore not referred to here as electrical spraying. In order to control and study electrical spraying more readily, it is usual to confine the actual spraying region to the tip of a capillary tube. The liquid to be sprayed is supplied to the capillary tube from a reservoir at a pressure insufficient to cause mechanical spraying. If the capillary tube is an electrical conductor, then only the liquid emerging from the tip is influenced by the external electric field. The electric field is produced by applying voltage between the conducting tube and a ground surface as shown in Fig 1. The capillary tube is usually held positive with respect to the ground surface in order to reduce field emission effects at the conducting tip.

Influence of Conductivity and Potential

When a liquid having a relatively high conductivity is subjected to the electric field at the tip of the conducting tube, a charge builds up on the liquid surface. This charge is attracted toward the ground plate, and if field emission

does not occur, a quantity of liquid may move away from the tip of the conducting tube as depicted in Fig 2.

When the influence of surface tension is overcome by a sufficiently large field, a large drop breaks away accompanied by several smaller droplets formed from the original interconnecting thread of liquid. The large drop carries a charge determined by the original surface charge, and its radius is determined by (but may be larger than) the radius of the conducting capillary tube.

At this point two situations can arise determined by the applied potential. These are presented here as case 1 and case 2.

Case 1 low potential Assume the situation in Fig 2c. The charged heavy drop moves toward the ground plate at a relatively low acceleration because of the low electric field. Its presence shields the liquid at the tip of the conducting tube, thus reducing the field, and allows the liquid to relax back to the shape shown in Fig 2a. The equipotential surfaces follow the shape of the liquid surface. Then, as the heavy drop continues on its way, the field builds up again at the tube tip. This creates another charged heavy drop, and the sequence shown in Fig 2 is repeated, etc. The large drops produced in this case have a relatively small specific charge.

Case 2 high potential Again assume the situation in Fig 2c. Now, however, the heavy drop has a higher acceleration toward the ground plate caused by the high potential. The liquid at the tip of the capillary tube cannot relax back to the shape of Fig 2a before the drop moves away, and so now there is a high field at the pointed end of the liquid. The electric field draws the point out still more until the field at the surface is sufficient to overcome the effect of surface tension. This action produces small charged droplets having a relatively large specific charge.

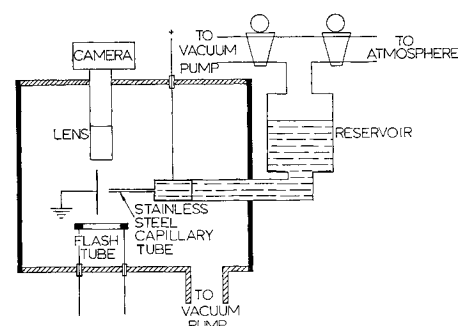


Fig 1 Schematic of the arrangement used to generate and photograph the charged liquid droplets

Presented as Preprint 63051-63 at the AIAA Electric Propulsion Conference, Colorado Springs, Colo., March 11-13, 1963; revision received January 17, 1964. This work was supported in part by National Science Foundation Grant NSF-G 19776 and in part by U. S. Air Force Grant AF-AFOSRG 107-63.

* Director, Charged Particle Research Laboratory

† Staff members, Charged Particle Research Laboratory

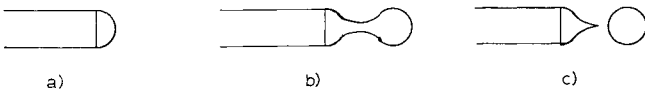


Fig 2 Consecutive stages in the development of electrical spraying

In both case 1 and case 2 it has been assumed that the liquid is a conductor. If the liquid has a low conductivity, charge may be removed from the surface more rapidly than it can be replenished through the liquid. In such a case, the equipotential surfaces will not follow the liquid surface but may follow very closely the capillary contours. Thus, the high fields will appear at the capillary "corner" as shown in Fig 3. Spraying of the liquid will then occur as a set of irregular sprays around the periphery of the capillary as shown in Fig 4. Almost no liquid will be sprayed along the capillary axis in this case. Spraying of this type can be produced using liquids such as 2-ethylhexyl phthalate (Octoil), which has a high volume resistivity. At suitably low potentials (with a given capillary diameter), Octoil sprays as a conductor, as discussed in cases 1 and 2. At higher potentials, Octoil sprays as an insulator. This behavior has been observed at atmospheric pressure as well as in a vacuum ($p \cong 10^{-6}$ torr).

Rayleigh's Theory

Rayleigh⁴ proposed a solution to the problem of instability of conducting liquid droplets. The method involved in Rayleigh's theory was based on the assumption that the equation for the radius of the spheroidal droplet at any time can be given by

$$r = a_0 + \sum_n a_n P_n(\mu) \quad (1)$$

where $a_n \ll a_0$ for all n , $P_n(\mu)$ is the Legendre polynomial of order n , $\mu = \cos\theta$, and a_n depends on time. Here θ is the polar angle (see Fig 5). One then finds the potential energies of the electric charge and surface tension, and the kinetic energy of the motion. Having done this, the Lagrangian equation of motion can be written. With the assumptions just given, the functions a_n are found to be the normal coordinates of the motion.

Application of Rayleigh's Theory

There is one essential difference between the foregoing treatment of Rayleigh and the case of fluid at the end of a spraying capillary tube. As shown in Fig 5, we have the additional constraint on the vibrating meniscus at the end of the capillary tube that, at $\theta = \pi/2$, $r = a_0$. The constraint forces us to modify Eq (1) assumed for the radius. We now assume that, at any time, the surface can be written as

$$r = a_0 + \sum_{n=1} a_{2n-1} P_{2n-1}(\mu) \quad (2)$$

This summation now extends only over odd harmonics in

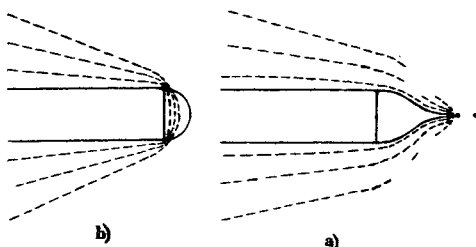


Fig 3 Equipotential surfaces (dashed lines) at end of capillary tube: a) conducting liquid, b) nonconducting liquid

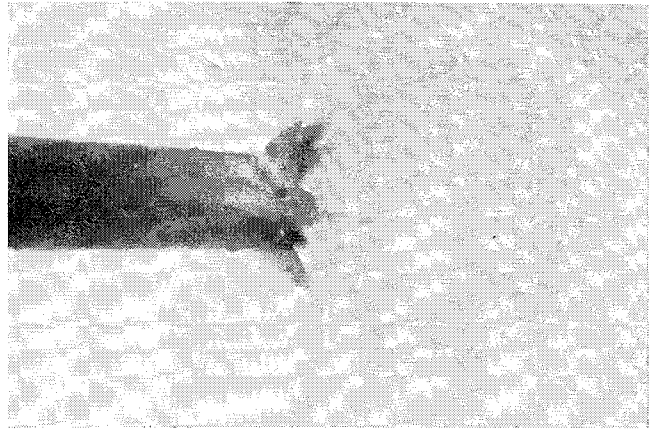


Fig 4 Photomicrograph of Octoil operating under high-field conditions (10 kv d c)

order to satisfy the additional constraint given in the foregoing

The volume of the hemisphere of moving liquid at the end of the capillary is given by

$$\text{volume} = \frac{2\pi}{3} \int_0^{\pi/2} r^3 \sin\theta d\theta$$

Performing the indicated integrations using Eq (2) we get

$$\tau = \frac{2\pi}{3} a_0^3 \left\{ 1 - 3 \sum \frac{(-1)^n (2n)! a_{2n-1}}{2^{2n} (n!)^2 (2n-1) a_0} + \sum (4n-1)^{-1} \frac{a_{2n-1}^2}{a_0^2} \right\} \quad (3)$$

where higher order terms in a_{2n-1} have been neglected. If a is the radius of a hemisphere with equivalent volume, then

$$a^2 = \left(\frac{3\tau}{2\pi} \right)^{2/3} = a_0^2 \left\{ 1 - 2 \sum \frac{(-1)^n (2n)! a_{2n-1}}{2^{2n} (n!)^2 (2n-1) a_0} + 2 \sum \frac{a_{2n-1}^2}{(4n-1) a_0^2} \right\}^\dagger$$

At this point let us assume that the volume of liquid at the capillary tip is constant. Therefore we are implicitly assuming that the instability occurs in a time which is short compared with the time required for appreciable amounts of fluid to flow through the capillary. Also, we are assuming that the a^2 given in the foregoing is a constant. This is a striking result, since it is composed of a summation of terms that can change with time. We may take this assumption to be another restriction on the magnitudes of the a_n 's.

The potential energy P of capillarity is equal to the product of the surface area and the surface tension γ . The surface area S is given by

$$\begin{aligned} S &= 2\pi \int_0^{\pi/2} r \sin\theta \left\{ r^2 + \left(\frac{\partial r}{\partial \theta} \right)^2 \right\}^{1/2} d\theta \\ &\cong 2\pi \int_0^{\pi/2} \left\{ r^2 + \frac{1}{2} \left(\frac{\partial r}{\partial \theta} \right)^2 \right\} d\mu \\ &= 2\pi \left\{ a_0^2 - 2a_0 \sum \frac{(-1)^n (2n)! a_{2n-1}}{2^{2n} (n!)^2 (2n-1)} + \sum \frac{(2n^2 - n + 1) a_{2n-1}^2}{4n-1} \right\} \end{aligned}$$

† Close examination of this equation shows that additional cross-product terms in a_{2n-1} may be involved in a^2 . However, inclusion of these terms drastically changes the Lagrangian. The resulting equations of motion would be coupled equations, and, since we seek uncoupled equations, we omit these terms without serious error.

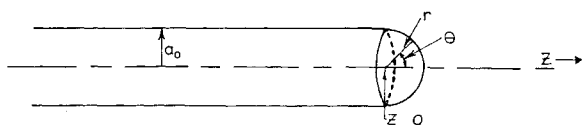


Fig 5 Geometry of capillary tube and liquid hemisphere

Therefore, the potential energy of surface tension is

$$P = 2\pi\gamma\Sigma \frac{(2n+1)(n-1)a_{2n-1}^2}{4n-1} \quad (4)$$

correct to second order in a_{2n-1} . This potential energy is taken with reference to a hemisphere of radius a as given in the foregoing

At this point we make the rather strong assumption that the potential distribution about the hemispheroid on the tip of the capillary tube is approximately the same as the potential distribution about a spheroid in free space⁷ provided $Z > 0$. The energy stored about such a charged spheroid in terms of the charge Q (in electrostatic units) on the spheroid is⁷

$$W = -\Sigma(2n-2)(Q^2/2a^3)a_{2n-1}^2(4n-1)^{-1}$$

correct to second order in a_{2n-1} . However, in our case, we make the additional assumption that only one-half the total charge on the sphere resides on our hemisphere. Therefore, we divide the foregoing energy expression by two. Furthermore, we replace Q/a by the potential on the capillary. The final expression becomes

$$W = -\Sigma(2n-2) \frac{V^2 a_{2n-1}^2}{4(300)^2 a (4n-1)} \quad (5)$$

In order to obtain the kinetic energy we assume that the spheroid is composed of a homogeneous inviscid incompressible fluid. The velocity potential then can be expanded in a harmonic series in the form

$$\psi = \Sigma_m \beta_m r^m P_m(\mu) \quad (6)$$

Comparing the radial velocity of the surface obtained from (6) with that obtained from (2), we find that, for m even, β_m is zero, and, for m odd,

$$ma^{m-1}\beta_m = \dot{a}_m \quad (7)$$

Since the kinetic energy is given by

$$T = \frac{1}{2} \rho \int v^2 d\tau = \frac{1}{2} \rho \int_0^1 \psi \frac{d\psi}{dr} a^2 d\mu \quad (8)$$

where v is the velocity of the liquid at a point, $d\tau$ is the volume element, and ρ is the density, we obtain from (6-8), correct to second order in a_{2n-1} ,

$$T = \Sigma_{n=1} \pi \rho a^3 (2n-1)^{-1} (4n-1)^{-1} \dot{a}_{2n-1}^2$$

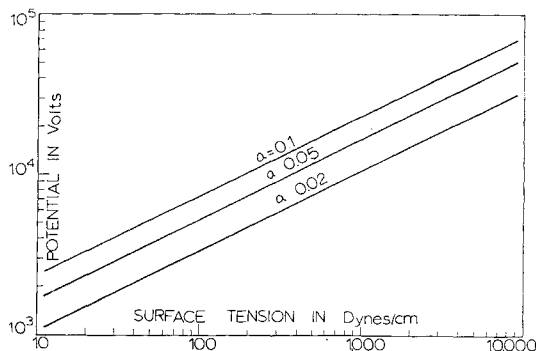


Fig 6 Minimum spraying potential vs surface tension with capillary radius as a parameter

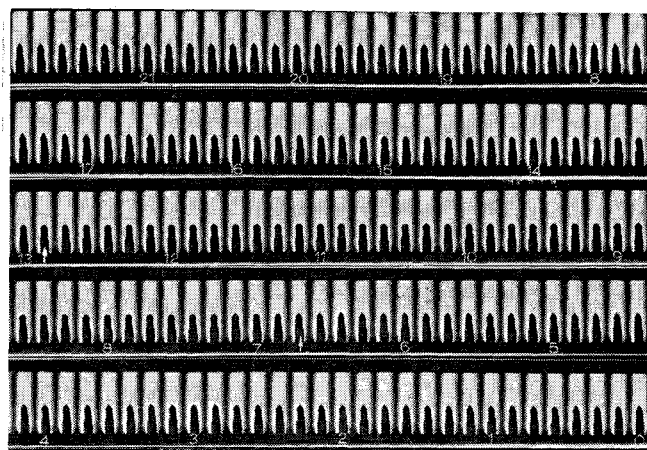


Fig 7 High-speed photographs of spraying glycerine. The film speed was 7000 frames/sec. The potential applied to the needle was 5 kv d.c. and was pulsed off for 6 msec. The arrows indicate the pulse duration. Time (in milliseconds) increases from right to left in each film strip.

The Lagrangian of the motion is

$$L = T - P - W = \Sigma_{n=1} \left\{ \pi \rho a^3 (2n-1)^{-1} (4n-1)^{-1} \dot{a}_{2n-1}^2 - 2\pi\gamma(2n+1)(n-1)(4n-1)^{-1} a_{2n-1}^2 + [V^2/4(300)^2 a] (2n-2)(4n-1)^{-1} a_{2n-1}^2 \right\}$$

Therefore, the equation of motion of the a_{2n-1} 's is

$$\ddot{a}_{2n-1} + \frac{(2n-1)(n-1)}{\rho a^3} \left\{ 2(2n+1)\gamma - \frac{V^2}{2\pi(300)^2 a} \right\} \times a_{2n-1} = 0$$

If

$$a_{2n-1} \propto \cos(\omega t + \delta)$$

then

$$\omega^2 = \frac{(2n-1)(2n-2)}{\rho a^3} \left\{ (2n+1)\gamma - \frac{V^2}{4\pi(300)^2 a} \right\}$$

Minimum Spraying Potential

When

$$(2n+1)\gamma < V^2/4\pi(300)^2 a \quad (9)$$

the surface becomes unstable because then ω is not a real number. Equation (9) allows us to determine the minimum

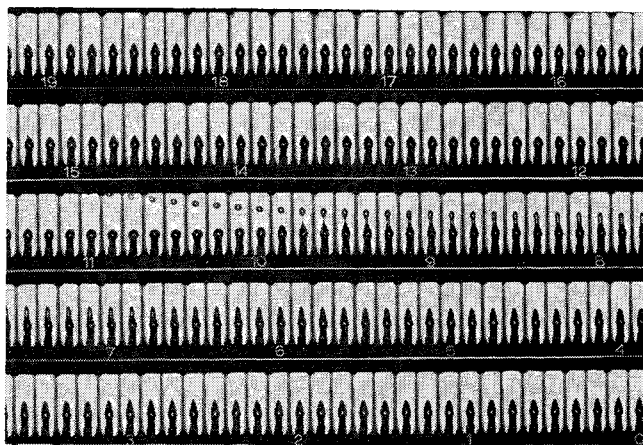


Fig 8 High-speed photographs of Octoil-S spraying at a potential of 4.7 kv d.c. The film speed in this sequence was 7900 frames/sec. Time (in milliseconds) increases from right to left in each sequence and from bottom to top.

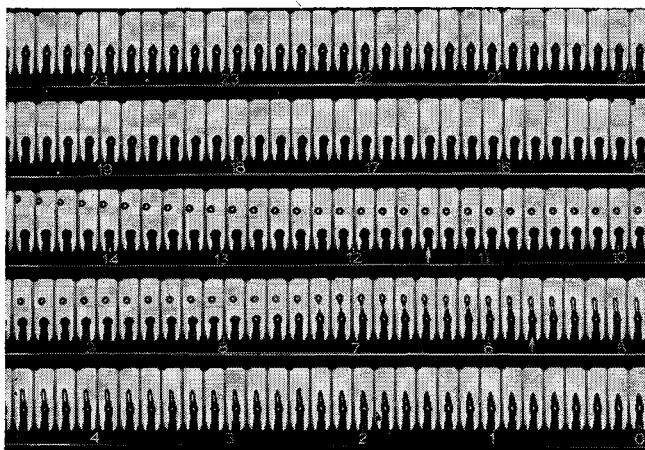


Fig 9 High-speed photographs of Octoil-S The film speed during this sequence was 6240 frames/sec. The potential was 4.7 kv d c and was pulsed to -5.3 kv d c for 6 msec. The arrows indicate the pulse duration. Time (in milliseconds) increases from right to left in each film strip.

spraying potential. If we substitute $n = 2$ (the lowest allowable value of n), we find that, if

$$\gamma < V^2/20\pi(300)^2a \quad (10)$$

then the surface of the liquid at the capillary tip will be unstable, and spraying of colloid particles will result. It should be noted that usually it requires more than the potential indicated by Eq (10) to start the spraying. However, this formula has been experimentally verified in that it indicates the minimum spraying potential.

Figure 6 is a graph of the minimum spraying potential vs surface tension with capillary radius as a parameter. It is assumed in Fig 6 that $a_0 \cong a$, which is correct to first order in the small quantities a_{2n-1} .

Photomicrographs

The charged-droplet beam was produced by means of a stainless-steel capillary tube held at a high potential variable from 1 to 10 kv. The arrangement was shown previously in

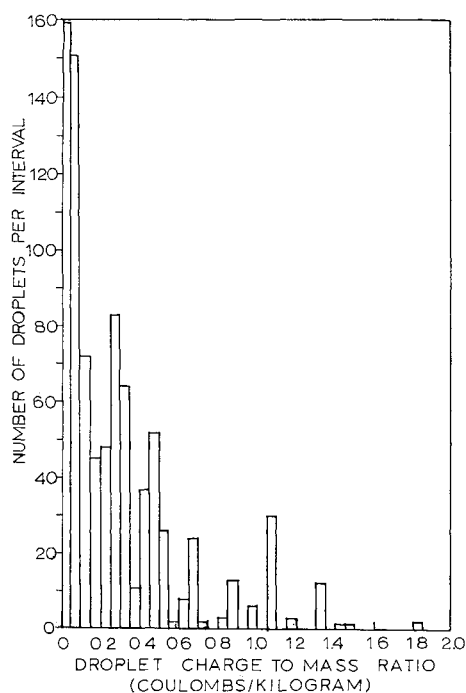


Fig 10 Specific charge distribution of Octoil

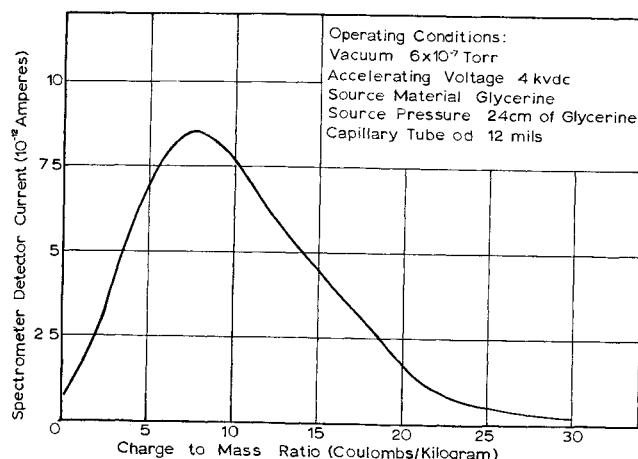


Fig 11 Specific charge distribution for glycerine

Fig 1. In order to take the series of high-speed photographs, the light from a carbon-arc lamp instead of the flash tube was focused on the capillary tip, and a microscope objective lens was placed in front of the camera shutter. The outside diameter of the capillary tube was 12 mils.

One series of frames taken of the capillary tip is shown in Fig 7. This sequence shows the induced relaxation and buildup of a charged glycerine beam when an applied voltage of 5 kv is pulsed off for 6 msec. The film speed for this sequence was about 7000 frames/sec. As is seen on the photographs, no droplets were emitted for approximately 11.5 msec. This time differential is considerably longer than the charge relaxation time σ of glycerine (which is on the order of $9 \mu\text{sec}$). It is thought that the time lag is due to the finite time required to build up sufficient charge on the liquid surface to overcome surface tension forces.

Figure 8 shows natural cycles of the two modes of operation of Octoil, namely, microscopic-sized charged-particle emission and macroscopic-sized charged-particle emission. Again the charge buildup of the liquid can be readily observed. Here, however, the buildup and relaxation of the liquid surface is natural in contrast to the previously discussed induced relaxation by means of potential pulsing. This is understandable in view of the fact that Octoil has a conductivity on the order of a millionth of that of glycerine. As a result of this low conductivity, the liquid tip experienced a slow buildup of charge which increased to the point of instability of the liquid. At this point, charged particles were emitted and this reduced the net charge at the liquid tip and caused the surface to relax to a stable stage again. Then the cycle repeats.

For this sequence of pictures the flow rate into the capillary tip was greater than the charged-mass flow away from the capillary. As a result, a slow accumulation of mass can be observed at the capillary tip. This phenomenon causes a large macroscopic droplet of low specific charge to be emitted. The field-shielding effect of the droplet on the relaxing connecting thread is observable in these pictures. The charged droplet may cause a field reversal between the droplet and the capillary causing the spray to collapse back into the source liquid surface. This phenomenon is shown more dramatically in Fig 9 where the applied 5 kv capillary voltage is pulsed negatively for 6 msec by the same magnitude of d c voltage. In this sequence, the thread forms a small drop, which is accelerated back toward the capillary. It should be noted, however, that the induced field reversal is strong enough to cause the large droplet to reverse direction during the negative pulse.

Figure 4 shows the behavior of Octoil under high-field conditions in which events are occurring so rapidly that charge transfer cannot take place at a rate sufficient to maintain an equipotential surface at the spraying tips.

Specific Charge

As a result of both the theoretical treatment and the photomicrographs, it appears that the emitted droplets do not all necessarily have the same radius or the same charge. It is anticipated, then, that there is a wide range of radii and of charges, which result in a distribution of specific charge.

One of the first series of measurements of individual droplet specific charge in vacuo was performed by Hendricks⁵. Using an experimental arrangement similar to Fig 1 with Octoil as the liquid and with a Faraday Cage as a single-particle detector, it was found that the specific charge distribution had a wide range of values and a maximum of about 0.06 coul/kg at an applied potential of 12 kv. The specific charge varied with potential, and the maximum of the distribution shifted to a higher value of about 1 coul/kg when the potential was increased. The specific charge also increased when the flow rate of the Octoil was restricted.

When liquid Wood's metal was used, maximum specific charge on the order of 10^4 coul/kg have been observed.

The histogram shown in Fig 10 shows the specific charge distribution for Octoil. This histogram was obtained by measuring individual specific charges. Specific charge has recently been measured using a quadrupole mass spectrometer or Massenfilter. A typical distribution for glycerine is shown in Fig 11.

The spread of values in the distribution of specific charge has been narrowed by dissolving ionic conductors such as antimony trichloride or tetra-n-butylammonium picrate in the Octoil or Glycerine.⁶

Conclusions

These pictures indicate that charged-droplet emission from high-field liquid surfaces is sporadic for some liquids. Earlier investigations⁵ of the specific charge distributions for many liquids have indicated that heavy charged particles as well as ions are emitted simultaneously from high-field points. However, the sporadic emission observed in the present work tends to support the theory that heavy charged particles and ion emission do not occur simultaneously, but occur at different levels of instability of the liquid surface.

References

- ¹ Langmuir, D. B., "Optimization of rockets in which fuel is not used as propellant," Ramo-Wooldridge Res. Lab. Rept. ERL-101 (September 1956).
- ² Stuhlinger, E., "Possibilities of electrical space ship propulsion," *Transactions of the Fifth International Astronomical Congress*, edited by F. Hecht (Springer, Innsbruck, Austria, 1955), 100-119.
- ³ Shelton, H., "Commentaries on the optimization of constant thrust electrical propulsion systems," Ramo-Wooldridge Res. Lab. Rept. ERL-LM-101 (1956).
- ⁴ Rayleigh, J. W. S., "On the equilibrium of liquid conducting masses charged with electricity," *Phil. Mag.* **14**, 184 (1882).
- ⁵ Hendricks, C. D., Jr., "Charged droplet experiments," *J. Colloid Sci.* **17**, 249 (1962).
- ⁶ Krohn, V. E., Jr., "Glycerol droplets for electrostatic propulsion," *ARS Paper* 2398-62 (March 1962).
- ⁷ Hendricks, C. D., Jr. and Schneider, J. M., "Stability of a conducting droplet under the influence of surface tension and electrostatic forces," *Am. J. Phys.* **31**, 450 (1963).